
Article:
Dorgham, A, Parsaeian, P orcid.org/0000-0001-8393-3540, Azam, A orcid.org/0000-0002-3510-1333 et al. (3 more authors) (2019) Single-asperity study of the reaction kinetics of P-based triboreactive films. Tribology International, 133. pp. 288-296. ISSN 0301-679X

https://doi.org/10.1016/j.triboint.2018.11.029

Single-asperity study of the reaction kinetics of P-based triboreactive interfaces

Abdel Dorgham*[a], Pourya Parsaerian[a], Abdullah Azam[a], Chun Wang[a], Ardian Morina[a], and Anne Neville[a]

[a]*Institute of Functional Surfaces, School of Mechanical Engineering, University of Leeds, Leeds LS2 9JT, UK*

Abstract: The reaction kinetics of zinc dialkyldithiophosphate (ZDDP) and ashless DDP antiwear additives were studied using in-situ single asperity AFM experiments. The results show that the ZDDP molecules decompose under high temperature and contact pressure following first order reaction kinetics ($n = 0.71 \pm 0.14$), whereas the DDP molecules follow a more complex fractional order ($n = 0.52 \pm 0.07$). The fractional order indicates that the decomposition process includes more side and intermediate reactions that consume part of the additive to form species, i.e. possibly volatile products, other than the antiwear phosphate glass on the contacting surfaces. In the case of ZDDP, the formation rate of the phosphate glass follows an equal exponential dependence on both temperature and contact pressure. However, in the case of DDP, it increases exponentially only over contact pressure and linearly over temperature. The findings of this study advance our understanding of the currently widely-used P-based antiwear additives and open future opportunities to develop new green alternatives with similar antiwear capabilities.

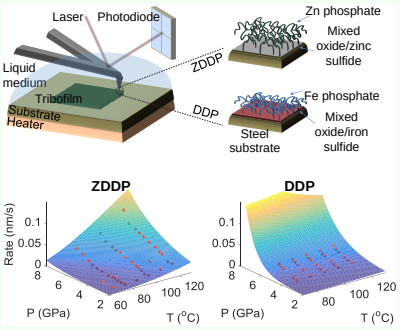

Keywords: *reaction kinetics, in-situ AFM, ZDDP, antiwear tribofilms, green lubricants*

Introduction

Phosphorus-based additives such as ZDDP and DDP are well-known to be highly reactive when sheared at high temperature between contacting surfaces (Figure 1) [1]. Initially, these additives adsorb to the rubbing surfaces with a maximum coverage when the ZDDP or DDP molecules are flat and their sulfur atoms lay near the surface. The reaction of the adsorbed molecules with the oxide layer on bare steel rubbing surfaces produces initially a mixture of zinc and iron sulfate in the case of ZDDP (Figure 1b) [2] and iron sulfate in the case of DDP (Figure 1c) [3, 4]. The sulfate species are quickly reduced into sulfides at the asperity contacts under the influence of high temperature and contact pressure [2, 5]. Subsequently, the P-additive molecules decompose completely to form layers of zinc phosphate of increasing chain length away from the substrate in the case of ZDDP [5], whereas in the case of DDP layers of short chain iron phosphate are mainly formed [6].

The formation of the phosphate layers on the rubbing surfaces led to the widespread use of the P-based additives in many industries due to their superior antiwear capability. The general consensus regarding the origin of the antiwear mechanism is that it can be due to i) the sacrificial nature of the phosphate layers at the contacting surfaces thus preventing adhesive wear [1], ii) the ability of phosphate layers to digest sharp particles worn from the contacting surfaces thus mitigating abrasive wear [7], iii) the ability of the additives to decompose peroxy radicals thus limiting surface oxidation [8], or iv) a combination of the previous mechanisms.

Apart from the many advantages of the P-based additives such as ZDDP, they have numerous disadvantages as well. For instance, they can increase micropitting of rolling contacts, which decreases their bearing life [9, 10]. In addition, the use of these additives in systems equipped with catalytic converters such as the exhaust system of vehicles can poison the catalyst due to the presence of sulfur and phosphorus, which leads to more harmful emissions [11]. Therefore, increasingly stricter environmental rules are introduced frequently on the allowed concentrations of P-based additives in the oil [12]. In order to find environmentally friendly alternatives with a good antiwear capability, first the decomposition reactions and kinetics of the superior antiwear P-based additives need to be better understood. The formation

*Corresponding author:
Abdel Dorgham (a.dorgham@leeds.ac.uk)

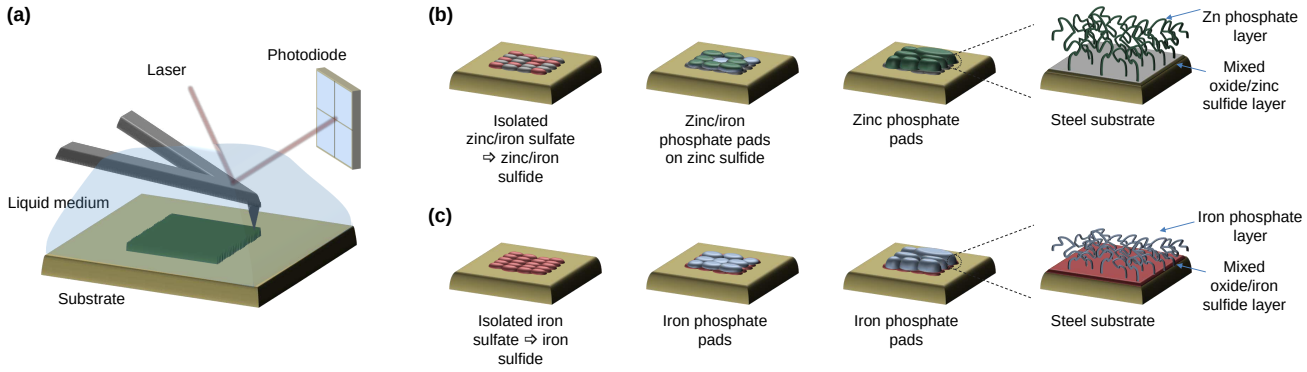

Figure 1. In-situ formation of ZDDP and DDP triboreactive films using a single-asperity AFM tests. a, Schematics of the in-situ AFM setup showing that the probe and steel substrate are fully submersed in oil. b and c, Growth steps of the ZDDP and DDP triboreactive films, respectively.

kinetics predetermine the thickness, tenacity, durability and ultimately the antiwear capability of the formed tribofilms.

Despite the extensive work to elucidate the antiwear mechanisms of P-based additives [13], little is known about the exact kinetics of their decomposition reaction to form protective phosphate-rich tribofilms under high temperature and rubbing. The main obstacle originates from the nature of the tribo-induced reactions that can follow different complex pathways. The reaction pathway changes depending on whether the base oil containing the antiwear additive may also contain adventitious impurities [14], other additives [15, 16], detergents [17] and dispersants [18]. The operating conditions [19] and compatibility between the additive and contacting surfaces [20] are also important factors.

The only available data regarding the rate of the decomposition reactions of P-based additives in base oil suggest that the ZDDP reaction initially follows a zeroth order, but after long sliding cycles starts to follow a more complex fractional rate of about 0.2 [1]. However, previous results suggested a first order reaction kinetics for the decomposition of materials of similar functional groups found in P-based additives, e.g. dimethyl and diethyl disulfide [21] and other groups under shear [22, 23].

Temperature and contact pressure appear to have an accelerating effect on the decomposition reaction of P-based additives and the formation rate of their protective tribofilms [1]. However, it is still not completely clear whether temperature and contact pressure have a combined additive effect, or one has a bigger effect than the other. Thus far, the influence of temperature and contact pressure has been considered to follow a chemo-mechanical Arrhenius-type model, which recently has been implemented in several studies for the case of ZDDP [1, 24]. This model, which in its basic form considers contact pressure to mainly reduce the activation energy of the reaction, assumes that the kinetics have exponential dependence on both temperature and contact pressure. However, the effect of the applied force is generally more complicated than temperature as not only the magnitude but also the speed, i.e. time, amongst other will have effect on the observed rate [22, 25, 26]. The applied force is expected to weaken the bonds more as the force quiescent time increases [25]. This indicates that the applied force has a time dependent effect, which can induce outburst of bonds rupture and therefore making the formation and removal rates time dependent. This effect has not been taken into account in the available experimental data related to the P-based additives despite its large potential impact.

This study aims at exploring the reaction kinetics of the P-based additives in more details taking into account the effect of speed and various levels of temperature (25–120 °C) and contact pressure (2–7 GPa) using in-situ single asperity AFM tribotests. These tests will allow us to study both the formation of the protective tribofilms over time and the evolution of their structures.

Materials and methods

The base oil used in this study is synthetic poly-α-olefin (PAO), which has a kinematic viscosity of 4 cSt at 100 °C. Using this base oil, two formulations were prepared; one contains secondary ZDDP and the second contains DDP. The amount of additive was added such that the phosphorus concentration in the base oil is fixed at 0.8 wt.%.

The in-situ tribological tests to form the ZDDP and DDP triboreactive films were performed using an atomic force microscope (AFM) - (Dimension Icon Bruker, USA), as shown in Figure 2a. The counterbodies, which slide against each other during the in-situ tests, were submersed in oil (Figure 2b) using an in-house designed high temperature liquid cell. The counterbodies consist of a sample made of AISI 52100 bearing steel, which has an average Rq roughness of 12 nm, and a silicon AFM probe (Rtespa 300, Bruker, USA), which has a nominal tip radius of 8 nm and a spring constant of 40 N/m. The in-situ AFM tests were performed using multi-pass

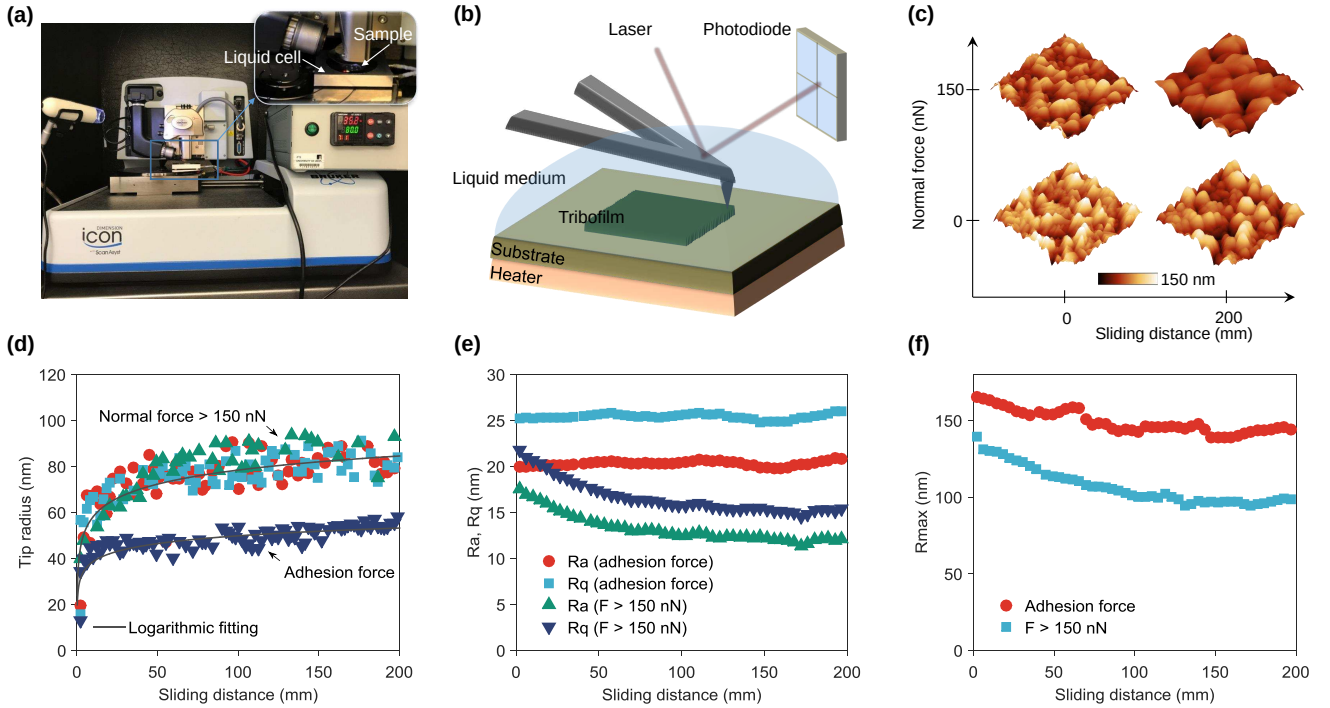

Figure 2. Materials and methods used to form ZDDP and DDP triboreactive films. a, AFM image showing the in-situ AFM setup consisting of Bruker Dimension Icon AFM and in-house made high temperature liquid cell. b, Schematics of the AFM showing that the probe and AISI 52100 bearing steel substrate are fully submersed in oil. c, Evolution of the topography AFM images over sliding distance of rough Ti substrate used for tip estimation under small adhesion force versus large contact force. Evolution of the estimated d, tip radius, e, R_a and R_q, and f, R_{max} over sliding distance under small adhesion force versus large contact force.

two-directional raster scans of an area of $5 \times 5\ \mu m^2$. After specific number of cycles, the tribotests were interrupted to capture high quality AFM images under low contact force < 100 nN of an area of $10 \times 10\ \mu m^2$, which is centered around the rubbed area.

To assess the wear behavior of the AFM tip, a Ti substrate of large roughness was scanned for different sliding distances as shown in (Figure 2c). The captured topography was largely affected by the normal load applied during scanning. The flattening of the rough features under the high contact force is mainly related to the large increase in the tip radius due to its progressive wear over sliding distance. The large tip overestimates the features of any size below the tip diameter. The evolution of the tip radius over the first 200 mm of sliding distance under two different loads using a standard Ti substrate of high roughness is shown in Figure 2d. The first chosen load was only due to adhesion force without any normal load applied whereas the second load was set at > 150 nN to represent a large normal force that could be applied during the in-situ AFM experiments. The results indicate that the tip initially has a radius of about 15 nm, which is close to its nominal value of 8 nm. The slight deviation can be related to the wear of the tip occurring during the tip engagement with the surface and during the calibration of the cantilever deflection sensitivity. The evolution of the tip size indicates that even after the first few millimeters of sliding, higher normal load leads to more wear of the tip, which is expected. Furthermore, the results indicate that the majority of wear occurs during the first 50 mm of sliding distance. The tip wear appears to follow a logarithmic trend until the tip radius reaches a steady state value after a sliding distance depending on the applied load, e.g. 25 mm in the case of adhesion force and 50 mm in the case of large contact force. This trend is in agreement with the results of Gotsmann and Lantz [27] and Liu et al. [28].

To quantify the flattening effect of the tip size on the features of the captured images, Figure 2e-f show the evolution of the measured surface properties based on the arithmetic average (Ra), Root Mean Square (Rms) and maximum (Rmax) roughness of the surface, as a function of the sliding distance. These statistical properties appear to be affected only slightly in the case of sliding under the adhesion force only. In contrast, when the applied load was increased to > 150 nN, a reduction by 30-40% was observed in the first 100 mm of the sliding distance, which is in agreement with the observed increase in the tip radius shown in Figure 2d.

Results and discussion

Growth of ZDDP tribofilms

Evolution of thickness and topography. The thickness and topography evolutions over sliding cycles of ZDDP tribofilms formed at 80 ^{o}C under 2.7, 4.5 and 5.7 GPa are shown in Figure 3a-d. For these different cases, the results indicate that initially the tribofilm thickness seems to increase linearly. However, after a certain number of sliding cycles, which depends on the applied contact pressure as shown in Figure 3e, the thickness starts to increase sharply with much faster kinetics. These observations are in agreement with the results of Gosvami et al. [1], which suggested that the growth of the ZDDP tribofilms undergoes two distinctive phases starting with a slow linear growth phase followed by a fast logarithmic phase. Figure 3e provides a comparison between the numbers of sliding cycles required before the growth rate of the tribofilms, formed under different contact pressures, to switch from the slow to fast growth kinetics. The results suggest that the increase in contact pressure reduces the needed cycles exponentially. For instance, at 2.7 GPa, 9000 cycles would be required as opposed to only 4000 cycles at 5.7 GPa. This indicates that the larger the contact pressure the faster the reaction kinetics of the ZDDP decomposition reactions.

Wear behavior. As rubbing continued, a decrease in the thickness of the formed tribofilms was observed (Figure 3a-c), which indicates that layers of the films were worn away. However, in few repetitions (e.g. Figure 3d), no removal cycles were observed. The topography images of the structure of the formed tribofilms indicate that the absence of removal is typically observed when the formed tribofilm is smooth and more compact. This resulted in a uniform linear growth of the tribofilm. On the other hand, when the formed tribofilm has a relatively high roughness, the growth phase proceeds with a much faster kinetics.

Interestingly, the tribofilm surface after every removal phase also appears to be rough, which seems to help accelerate a subsequent fast formation phase in which a large increase in the tribofilm thickness was observed over a small number of sliding cycles. The extra energy for this fast growth can originate from the broken dangling bonds of the undercoordinated atoms [29] and the creation of nascent surface of high reactivity during the preceding removal cycle [30]. If the tribofilm is initially smooth, no hastened formation would occur and thus no removal (Figure 3c). This steady formation results in a more compact tribofilm as it takes more time to grow and thus steady local reconfigurations are possible leading to a better accommodation of the newly formed layers and thus high compactness. However, the hastened formation produces thicker but less compact tribofilm layers that can be removed easily under shear. This is evident by noticing the striking similarity between the topography of the tribofilm just before the fast formation and after the removal. This indicates that the formation and removal cycles can be repetitive (Figure 3a-c), i.e. the more the tribofilm removal, the rougher the surface and the more the energy available for the next formation phase and consequently the faster the tribofilm formation.

Accumulated growth behavior. The effect of contact pressure can be further examined by studying its effect on the same tribofilm as it forms. This gives a better understanding of the effect of not only the contact pressure but also the substrate and its hardness and elastic modulus on the tribofilm formation. Figure 3f shows the evolution of the tribofilm thickness over different contact pressures ramped in the same in-situ tribotest. The data shows clearly that the formation rate increases over the contact pressure. The growth rate over sliding cycles was the same whether the contact pressure was applied to the steel surface directly or to the surface covered by a thin layer of tribofilm. The data provide two important findings.

First, the substrate effective hardness and elastic modulus felt by the AFM tip are not altered due to the presence of the ultra-thin tribofilms of $<$ 100 nm thickness. If this was not the case, the tribofilm growth rate should have been reduced as the tribofilm grows because the increased deformation should have increased the contact area and thus decreased the effective contact pressure.

Second, there is a pseudo steady-state thickness reached under 7.3 GPa of contact pressure. Under this pressure, it was expected that the tribofilm should keep growing but instead it reached a limited thickness after which no apparent growth was observed. The reason behind this steady-state condition can be related to the combined effect of the tribofilm deformation and the equilibrium between the tribofilm formation and removal. If removal was the only dominant process, then a sharp decrease in the tribofilm thickness should be observed. However, as the contact pressure is extremely severe, i.e. enough to wear the steel surface, the soft tribofilm can be easily removed but at the same time the high stresses are enough to accelerate the decomposition process to a great extent as to counteract the thickness-reducing processes of deformation and wear.

Effect of sliding speed. The changes in the growth rate of the ZDDP tribofilms formed at 80 ^{o}C and 7.3 GPa as a function of the scanning speed and sliding time per cycle are shown in Figure 4a. The results show that the speed does impact the reaction kinetics. However, the apparent increase in the formation rate over speed is primarily related to the decreased sliding time per cycle, as shown on the same Figure 4a rather than a genuine effect of the speed or shear rate. This is further confirmed in the inset of Figure 4a, which shows that if the growth rate is measured per cycle instead of per time, the speed has a negligible effect on the kinetics. This is somewhat expected as Clasen et al. [31] using the micro-

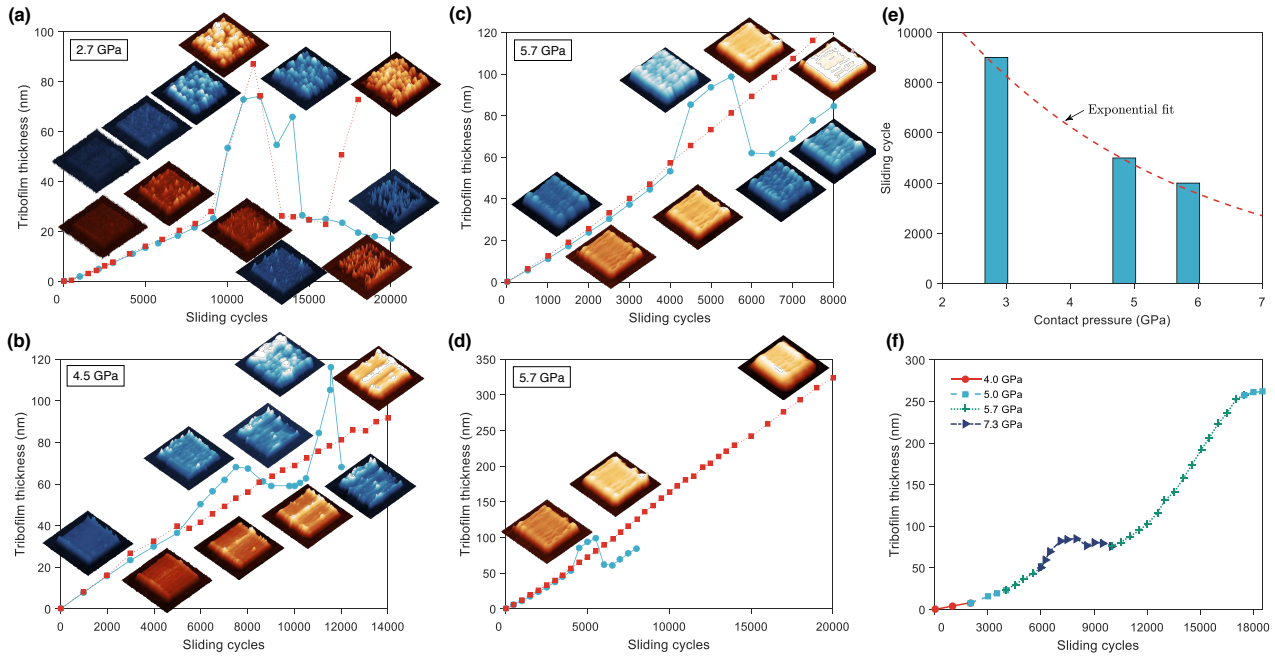

Figure 3. Effect of contact pressure on the growth of ZDDP triboreactive films formed at 80 ^{o}C. a, b, and c, Evolution of the thickness and structure of the formed films at 2.7, 4.5 and 5.7 GPa, respectively, over rubbing time after two repetitions. d, Evolution of the films formed at c, for longer rubbing cycles. e, Number of sliding cycles required before the growth rate of the tribofilms formed under different contact pressures to switch from the slow to fast growth kinetics. f, Evolution of the thickness of the triboreactive films over sliding cycles while ramping the contact pressure from 4.0 to 7.2 GPa at 80 ^{o}C.

gap rheometer showed that the shear stress in the boundary lubrication regime is independent of the shear rate and depends only on the friction coefficient, which is constant in this regime, and the applied normal force on the contacting asperities, which was constant during the in-situ tribotests at the various tested speeds. This is also in line with the results of Shimizu and Spikes [26], which showed that in the mixed sliding and rolling condition, the formation rate of the ZDDP tribofilm is less sensitive to the exact SRR. Therefore, this indicates that shear stress rather than the rate is the controlling parameter. However, they interpreted the data as the rubbing time is far more important than the sliding distance.

Our data seem to suggest that in the boundary lubrication regime the growth rate is less sensitive to the sliding speed and is only dependent on the sliding cycles. This is an interesting result as it indicates that the growth occurs cumulatively in a layer-by-layer fashion, i.e. every rubbing cycle regardless of its timing adds one layer of a certain thickness depending on the other operating conditions of temperature and contact pressure.

Effect of contact pressure and temperature. The growth rate of the ZDDP tribofilms formed at 80 ^{o}C can change over the applied contact pressure as shown in Figure 4. The data indicate that within the tested range of contact pressures, i.e. 2-6 GPa, shown in Figure 4a, the tribofilm growth rate increases linearly with a rate of 0.027 nm/GPa.s. The only available data similar to this work are the ones of Gosvami et al. [1], which are plotted in the same Figure 4a for comparison. The shift in data is mainly related to the uncertainty in contact pressure. In agreement with our results, the previously reported data seem to follow a linear trend with a similar rate of 0.033 nm/GPa.s. It is worth mentioning that Gosvami et al. [1] suggested that their data follow three distinct phases, i.e. i) initial slow growth below 3.5 GPa, ii) exponential growth from about 3.5 to 5.0 GPa and iii) steady-state equilibrium of formation and removal at high contact pressures above 5.0 GPa.

To verify whether the tribofilm growth follows a linear or exponential growth, a wider range of contact pressures up to 7.3 GPa was tested at 80 ^{o}C and the results are shown in Figure 4b. The whole set of data appears to follow a continuous exponential growth without any apparent steady-state phase. This is contrary to the results of Gosvami et al. [1]. If their steady-state argument can be neglected then their whole set of data can also be fitted with a single exponential growth model, with some variations due to the uncertainty in contact pressure, without the need to divide it into three phases as discussed before.

To confirm the validity of the single exponential fit argument, the growth rate was followed over a combination of

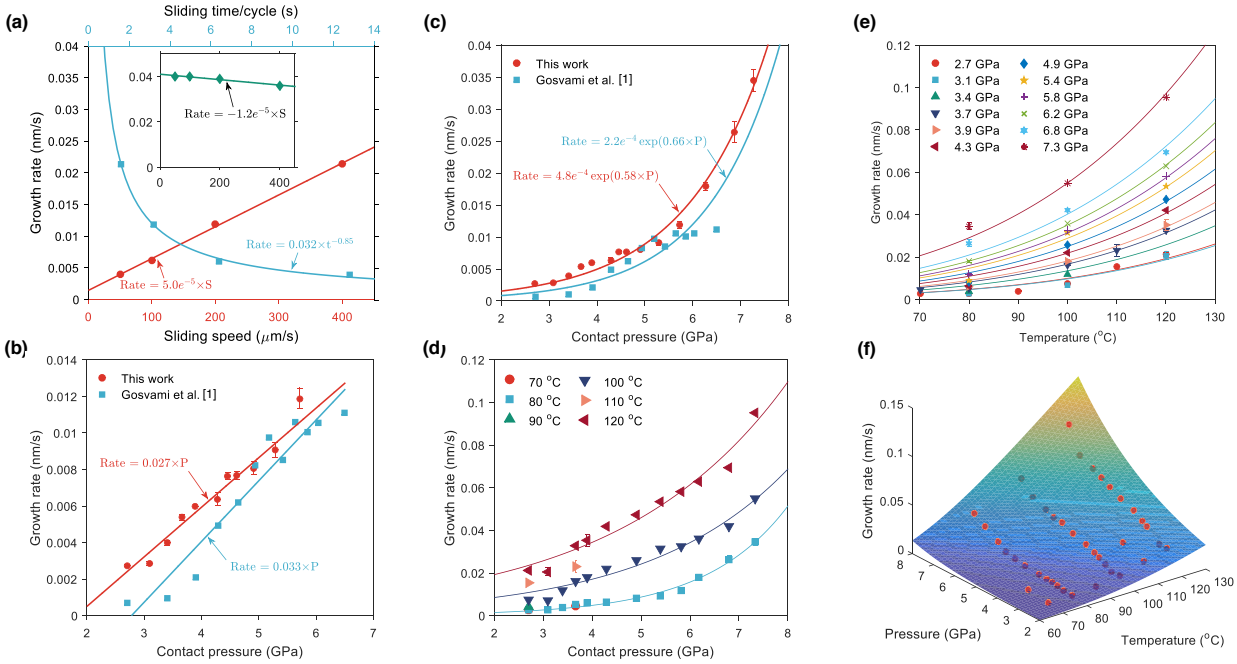

Figure 4. Effect of speed, temperature and contact pressure on the formation kinetics of ZDDP triboreactive films. a, Effect of sliding speed on the growth rate of the films formed at 80 ^{o}C and 7.3 GPa. The inset shows the effect of sliding speed on the growth rate if measured per cycle instead of per time. b and c, Linear and exponential effect, respectively, of contact pressure on the growth rate of the films formed at 80 ^{o}C. The results of Gosvami et al. [1] were plotted for comparison. d, e, and f, Evolution of the growth rate under different contact pressures and temperatures. The 3D surface in f, was generated using the chemo-mechanical Arrhenius-type model described in Equation 1.

various contact pressures (Figure 4c) and temperatures (Figure 4d). The results suggest that the whole dataset can be fitted using a single exponential fit. Furthermore, the data suggest that the higher the temperature or contact pressure, the higher the increase in the growth rate, which seems to follow an exponential trend.

The similar effect of temperature and contact pressure on the growth rate of the ZDDP tribofilms confirms their accelerating effect on the additive decomposition process [24, 32]. This suggests that the decomposition process of the ZDDP is thermally and mechanically assisted process, which can be activated by the availability of either shear or heat [32]. The synergy of these two factors on the growth rate of the ZDDP tribofilm is demonstrated in Figure 4f. For instance, the growth rate can be increased tenfold from 0.002 nm/s, at 70 ^{o}C and 2.7 GPa, to about 0.02 nm/s by increasing either the temperature to 120 ^{o}C or the contact pressure to 7.3 GPa. Therefore, the effect of temperature and contact pressure seems to be an additive effect as can be seen by the imaginary diagonal line in Figure 4f between temperature and contact pressure manifested by the maximum growth rate when the two are both maximum.

Growth of DDP tribofilms

The evolution over sliding cycles of the thickness and topography of DDP tribofilms formed at 80 ^{o}C and various contact pressures, i.e. 3.9, 4.3 and 5.2 GPa, are shown in Figure 5a-c, respectively. Similar to the case of ZDDP, the DDP results show a clear accelerating effect of contact pressure on the tribofilm growth rate. During the first 500 cycles, the formation rate increased from 0.005 nm/s at 3.9 GPa to about 0.018 nm/s at 5.2 GPa. As rubbing progressed, the tribofilm growth seems to enter a second phase of faster formation.

During the slow and faster formation phases, the formed DDP tribofilms did not show any removal as opposed to the case of ZDDP where the tribofilm formation was continuously interrupted by removal cycles. This can indicate that either the DDP tribofilm is more durable and tenacious than the ZDDP tribofilm or the removal cycles occur primarily after the tribofilm reaches a certain large thickness.

The evolution of the growth rate of the DDP tribofilm over a wide range of contact pressures and temperatures is shown in Figure 5d-f. The data indicate that the tribofilm growth rate increases exponentially over contact pressure, whereas it grows linearly over temperature. The more prominent effect of contact pressure implies that, above a certain threshold

of temperature, shear stress only is enough to cause a complete decomposition of the DDP additive to form a protective tribofilm. Increasing the temperature further does not have a potent effect as opposed to the case of ZDDP, which suggests different reaction pathways with different energy barriers.

Estimation of the activation energy

The accelerating effect of temperature and contact pressure on the decomposition reaction of P-based additives suggests that the reaction kinetics follow a chemo-mechanical Arrhenius-type model, which recently has been implemented by several studies for the case of ZDDP [1, 24]. This model in its general form reads:

$$k\,(T,P) = A\left[\exp\left(-\frac{E_a\,(P)}{K_{\mathrm{B}}T}\right)\right] \tag{1}$$

where A is the pre-exponential constant in the Arrhenius equation depending on the attempt frequency that is of the same order as the atomic vibration and the lattice parameter, K_{B} is the Boltzmann constant, T is the absolute temperature and E_a is the activation energy, which considering the second-order effects of the shear stress on the shape of the energy profile, can be given by [33]:

$$E_a\,(P) = E_0 - \mu P A_r \Delta x + \frac{\mu^2 P^2 A_r^2}{2}\,(\xi_{\mathrm{I}} - \xi_{\mathrm{T}}) \tag{2}$$

where E_0 is the nominal activation energy at no applied contact pressure (P), μ is the friction coefficient, A_r is the reactant area at which the contact pressure is applied, Δx is the activation length from the reactant state at $x = 0$ to the transition state along the reaction coordinate, ξ_I and ξ_T are the curvature values of the initial and transition states along the reaction coordinate, which can be given as follows:

$$\xi_{\mathrm{I}} = \frac{2\Delta x^2}{E_0\pi^2}\left(\frac{1+r}{1-r}\right)^2 \tag{3}$$

and

$$\xi_{\mathrm{T}} = -\frac{2\Delta x^2}{E_0\pi^2}\left(\frac{1-r}{1+r}\right)^2 \tag{4}$$

where $|r| \leq 1$ is the potential shape parameter, e.g. $r = 0$ represents a gradual transition from the reactant to the transition state, whereas $r = 1$ represents a sharp step like transition. This parameter is not known although a priori assumptions can be made. For instance, previous experimental results [1, 24] suggested that the contact pressure reduces the nominal activation energy of the ZDDP decomposition reaction linearly, which indicates that within the experimental certainties: $r < 0.7$ [33]. It follows that the higher order quadratic term of Figure 2, which consists of small quantities multiplied and all raised to the power of two, is likely to be negligible.

To fit Equations 1 and 2 to the experimental data, we need to make few assumptions. First, the pre-exponential factor, A, can be assumed to represent the frequency at which the reactant molecules cross the energy barrier into the transition state along the reaction coordinate. Considering that the distance from the reactant to the transition state is Δx and the molecules speed to be equally given by:

$$\nu = \sqrt{\frac{8k_{\mathrm{B}}T}{\pi m_e}} \tag{5}$$

where m_e is the effective mass, then the molecule frequency can be given by:

$$f_{\mathrm{a}} = \alpha\frac{\nu}{\Delta x} = \frac{\alpha}{\Delta x}\sqrt{\frac{8k_{\mathrm{B}}T}{\pi m_e}} \tag{6}$$

where α is a correction factor for the uncertainties related to the determination of both ν and Δx, which can be limited to $\pm 10\%$ of the nominal frequency value. The above relation is consistent with the oscillation frequency of the bond that is broken from the reactant, which is of the order:

$$f_{\mathrm{a}} \approx \frac{k_{\mathrm{B}}T}{h} \approx 10^{13}\ \mathrm{s}^{-1} \tag{7}$$

where h is the Plank constant.

The second assumption is related to the adsorption of the ZDDP molecules to the metal surface. This can be assumed to occur with a maximum coverage when the ZDDP or DDP molecules are flat on the surface, which means that their sulfur atoms lay near the surface. This is supported by the results of several previous studies [5, 34, 35], which indicated that the concentration of sulfur chemisorption products is higher on the steel surface as compared to the bulk of the formed tribofilm. This suggests that the decomposition of ZDDP or DDP molecules starts with their sulfur atoms near the surface, which is consistent with our proposed assumption. Thus, considering the standard structure of the ZDDP or DDP with average bond length of 2 Å [36], it follows that the effective area A_r can be taken as 1.0 nm^2 per ZDDP molecule [24] and 0.5 nm^2 per DDP molecule, i.e. half the one of the DDP.

The third assumption is related to the friction coefficient μ, which can be taken as 0.1 such that it matches the average value for the ZDDP and DDP tribofilms obtained using ex-situ pin-on-disc rig.

The fit of Equations 1 and 2 to the experimental data starts with three fitting parameters, i.e. α, E_0 and Δx while ignoring the second quadratic term of Equation 1. This is necessary for two reasons. First, in order to accurately estimate Δx and second, to be able to assess the significance of the quadratic term when compared to the results without including it. The fitting results are shown in Figures 4 and 5 for ZDDP and DDP, respectively. Same fit was obtained with and without the quadratic term, which indicates that the decomposition

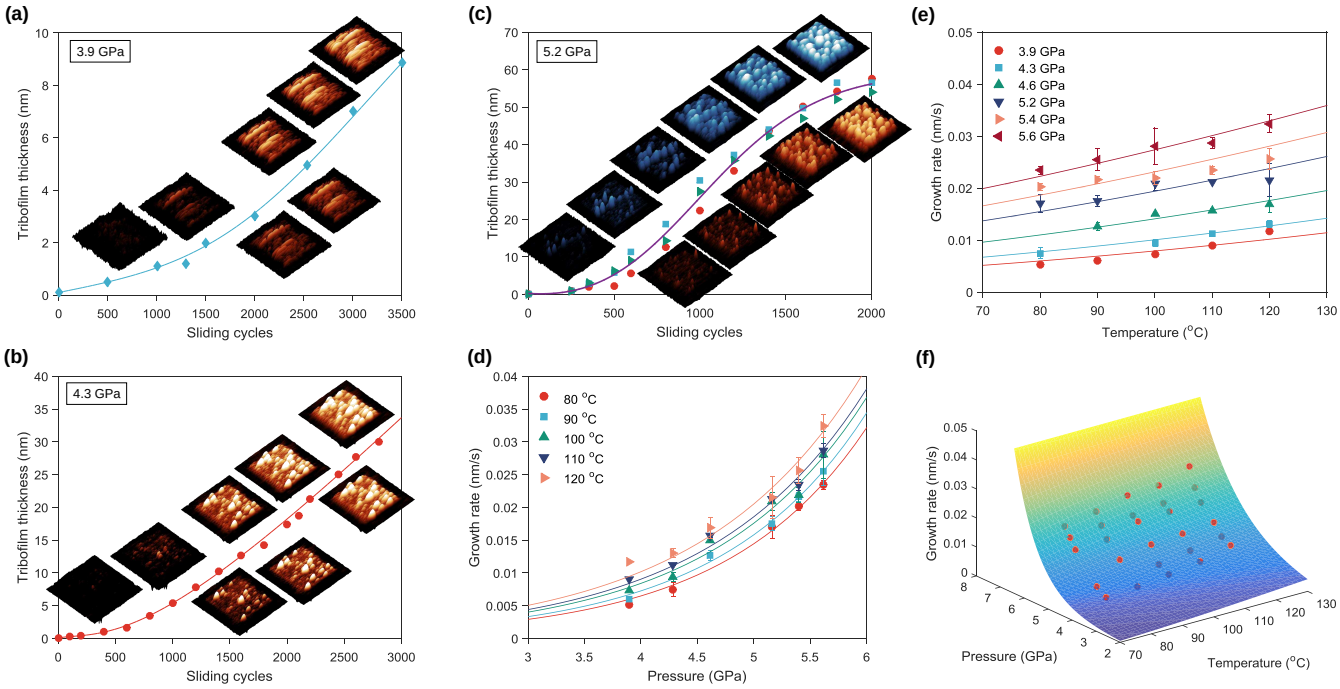

Figure 5. Effect of contact pressure and temperature on the formation kinetics of DDP triboreactive films. a, b, and c, Evolution of the thickness and structure of the formed films at at 80 ^{o}C and 3.9, 4.3 and 5.2 GPa, respectively, over rubbing time after two repetitions. d, e, and f, Evolution of the growth rate under different contact pressures and temperatures. The 3D surface in f, was generated using the chemo-mechanical Arrhenius-type model described in Equation 1.

reaction has the familiar Sine-Gordon (SG) potential rather than a step-like potential. This is confirmed by noticing the linear decrease of the activation energy E_0 over the contact pressure even when extrapolated to zero pressure, as shown in Figure 6. Such a behavior suggests a small $r \rightarrow 0$, which is also suggested by the numerical results of Tysoe [33].

The correction factor α for the uncertainties related to the determination of the attempt frequency, f_a, was found to be in the range of 10^{-2} to 1.0 for ZDDP and in the range of 10^{-5} to 10^{-3} for DDP over the entire tested range of pressure and temperature. The low values obtained in the case of DDP are a direct result of the linear rate increase over temperature compared to the exponential increase over contact pressure. This causes the pre-exponential factor, A, to be much less the expected value at 10^{13}. Similar deviation from this value was also found by Gosvami et al. [1] for the case of ZDDP.

The activation energy values for ZDDP range from 35 to 43 kJ/mol, whereas for the case of DDP range from about 10 to 25 kJ/mol, which are nearly half the value found for the ZDDP additive. The range of activation energy is consistent with the recent results of Gosvami et al. [1] of similar in-situ AFM tribotests and the results of Zhang and Spikes [24] of the ZDDP additive decomposing in viscous fluids using shear only and assuming no direct asperity-asperity contacts.

The smaller energy barrier, E_0, of DDP compared to ZDDP suggests that the decomposition reaction of DDP is more susceptible to contact pressure than the one of ZDDP. This indicates that the lack of zinc cations within the DDP molecules results in weaker overall bonds. Nonetheless, this does not warrant a faster reaction rate as it can be significantly affected by the activation length, which constitutes the rate-force dependency.

The activation length in the case of DDP was found to be about 0.8 Å, which is nearly fourfold the one found in the case of ZDDP, i.e. 0.2 Å. These values are consistent with the ZDDP results of Gosvami et al. [1] of 0.35 Å and other previously reported data in the literature for other materials but using a similar model [25, 37]. The reported values are feasible for the fitted atom-by-atom decomposition model that implies the activation lengths to be less than the length of the bond to be broken. On the other hand, the ZDDP results of Zhang and Spikes [24] suggested activation length of about 1.8 Å, which is of a relative order to the average bond length of 2 Å found in the ZDDP molecule [36].

Several factors might have contributed to the wide disparity in the reported activation length values. First, the different operating conditions between our single asperity AFM tribotests in the boundary lubrication regime and the conventional experiments of Zhang and Spikes in the elasto-hydrodynamic lubrication (EHL) regime.

Second, the limited range of contact pressures used to fit the data of Zhang and Spikes, which can result in misleading

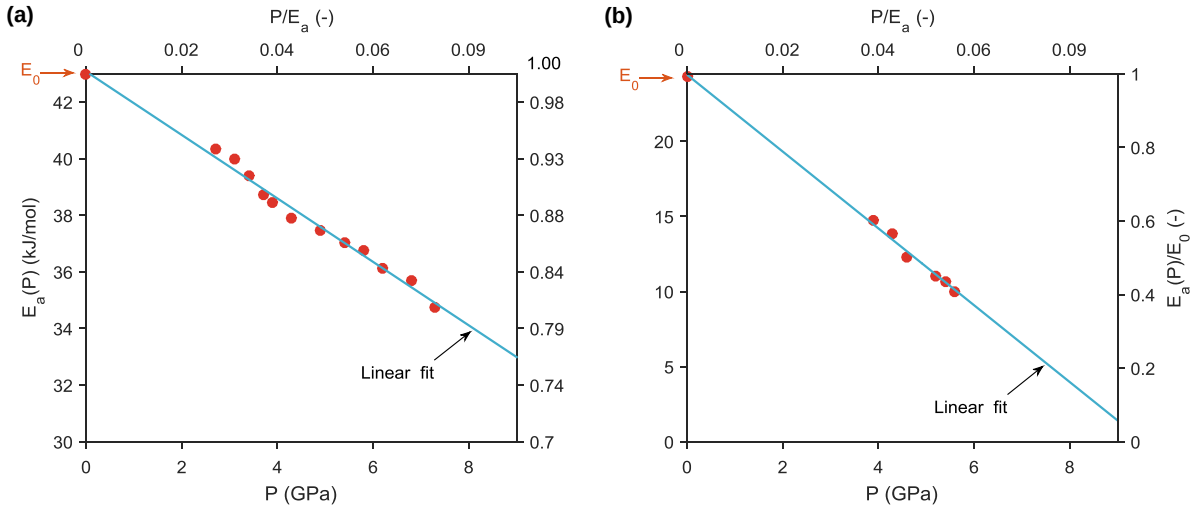

Figure 6. Evolution of activation energy E_a of the growth of a, ZDDP and b, DDP triboreactive films over contact pressure.

results by not capturing the complete but part of the formation trend.

Third, the original chemo-mechanical Arrhenius-type model suggested by Gotsmann and Lantz [27] is typically applied when the shear stress is taken to act on the bonds directly. However, the way the model implemented here is by taking the average shear stress to be equal to the applied contact pressure multiplied by the friction coefficient. The oversimplification of the complex flow within the contact can bring large errors in estimating the activation energy and its length. It is worth noting that Zhang and Spikes assumed that no direct contact exists between the sliding counterbodies as their experiments were conducted in the EHL regime. However, they considered the shear stress in a similar way to our treatment. Again, this is an overestimation rather than actual consideration.

Fourth, for the used Arrhenius kinetics model, the applied force is expected to weaken the bonds more as the force quiescent time increases due to the sharp decrease in the lifetime of the bond τ by several orders of magnitude [25], i.e. $F \propto 1/\tau$. This indicates that the applied force has a time dependent effect, which can induce outburst of bonds' rupture and therefore making the formation/removal rate constant k time dependent. However, despite its potential large impact, this effect has not been taken into account in the available experimental data related to the ZDDP additive. Nonetheless, it is worth noting that there are several models proposed to take into account the effect of sliding speed. For instance, the models of Briscoe and Evans [38] and Sang et al. [39] consider the effect of low and high speeds, respectively, on the shear stress at the interface and how it can affect the observed nanoscale friction. More recently, Tysoe [33] proposed a model to account for the velocity effect on the tribochemical reactions. The model is based on assuming that the energy barrier is time dependent and convoluted in the sliding velocity, thus the reaction rate can be found as follows:

$$\ln k\,(v) = \ln k_0 + \frac{\Delta x}{k_B T}\left[\frac{2F^*}{\pi} + \frac{2k_B T}{a}\ln\left(\frac{\nu}{aP}\right) - \frac{2}{a}\Delta E \ln\left(\frac{t_c \nu}{a}\right)\right] \tag{8}$$

where k_0 is the thermal reaction rate, ν is the sliding velocity, t_c is some characteristic time such that $t_c\nu/a \gg 1$, P is a factor related to the sliding transition over the energy barrier, ΔE is the change in the initial potential minimum due to sliding, $F^* = \pi E_0/a \gg F$ is the maximum force that can cause spontaneous sliding, E_0 and a are the height and periodicity of the energy potential. The terms inside the square brackets represent the applied force. Therefore, the model requires two fitting steps; one for the force to find the unknown parameters: F^*, a, P, and t_c and the other is for the whole rate equation in order to find the unknown Δx. In the case the change in the energy minimum, Δx, is smaller than the thermal energy, $k_B T$, which is expected to be almost always the case, the model predicts that increasing the sliding velocity would result in increasing the reaction rate. This is because the original formulation was designed to accommodate the observation that at small sliding speeds, where slip-stick friction occurs, increasing the speed results in a logarithmic increase in the atomic lateral force, i.e. atomic friction, leading to lower activation energy barrier [40, 41]. However, this does not hold true for micro- and macroscopic friction at high sliding speeds like the one used during the in-situ AFM tribotests. Furthermore, Equation 8 is in contrast with our previous discussion that the longer the quiescent time of the applied force, the weaker the bonds and thus the larger the reaction rate. A more appropriate treatment would rely on the reduction caused on the activation energy as the force is applied, which can be assumed a monotonically increasing time dependent effect, e.g. following a square-root dependence. Thus, the external force terms in Equation 2 can be

modified, as follows:

$$E_a(P) = E_0 + \left[\mu P A_r \Delta x + \frac{\mu^2 P^2 A_r^2}{2}(\xi_I - \xi_T)\right]\left(1 + \sqrt{\frac{\Delta x}{\nu t_c}}\right) \quad (9)$$

Fitting this equation is straightforward and based on the speed of 400 μm/s, it yields insignificant contribution of speed to the applied force, i.e the last term $\ll 1$. This is consistent with our results (Figure 4a) that the scanning speed per se does not impact the growth rate.

Fifth, under certain harsh conditions of high temperature and contact pressure, the severity at the contacting interface causes distortion to the structure of the transition state, i.e. the shape of the energy potential [40, 41]. As the decomposition reaction is endothermic, Hammond's postulate [42], which describes the structure of the transition state along the reaction coordinate, suggests that the energy of the transition state would be closer to that of the products than that of the reactants. In this case, the harsh conditions might alter this state such that the energy minimum in the reactants state to the transition state along the reaction coordinate becomes smaller with possible alteration to the relative energy difference as well [33]. Nonetheless, it is worth noting that this effect is not probable within our in-situ tested conditions as the contact pressure is not large enough to cause any alteration to the structure of the energy potential. Furthermore, if any alteration occurs, the activation length is expected to be shortened rather than elongated.

Sixth, the possible different types of the ZDDP additives, e.g. primary, secondary or a mixture of the two among others, used in the two cases though not expected to have any significant effect.

Estimation of reaction order

To find the order of the ZDDP and DDP decomposition reaction to form protective tribofilms on the shearing interfaces, the following equation for the nth order reaction rate can be used [1]:

$$\frac{1}{[V]^{n-1}} = \frac{1}{[V_0]^{n-1}} - (n-1)\,kt \quad (10)$$

where n is the reaction order, k is the reaction constant, V_0 and V are the tribofilm volumes at the beginning of the tribotest and at any time t, respectively. The initial volume of the tribofilm, V_0, can be taken as zero.

It should be noted that the above equation is suitable to estimate the reaction order only in the case of considering the changes of the reactants, i.e. additive concentration, or the products, i.e. the formed species of the tribofilm presumably phosphate species. As this information cannot be assessed during the AFM in-situ tribotests, the volume of the products will be considered instead of the concentration. This is a rough estimation but still feasible under the assumption that the thicker the tribofilm the larger the phosphate concentration.

As discussed before, the tribofilm formation follows a single exponential rate (Figures 4 and 5) as opposed to the suggestion of Gosvami et al. [1] that it undergoes two distinctive phases starting from a slow linear growth phase followed by a fast logarithmic phase. For comparison purposes, our data will be fitted assuming two phases in order to have a parallel comparison with the available data in the literature. This would not affect the conclusions as the first linear fit can always be ignored and the second exponential fit be extended to the whole dataset.

For the case of ZDDP, the reaction order was estimated by fitting Equation 10 to the growth evolution data obtained at three different contact pressures, i.e. 2.7, 4.5, and 5.7 GPa (Figure 4). The fitting results indicate that, regardless of the applied contact pressure, the slow linear phase of the tribofilm formation follows a zero reaction order with $n = 0.073 \pm 0.10$. On the other hand, the fast logarithmic growth phase of the tribofilm appears to follow approximately first order reaction kinetics with $n = 0.71 \pm 0.14$. As mentioned earlier, the entire dataset can be fitted using first order kinetics without the need of the initial zero order rate. The fitting results are in line with several previous reports suggesting a first order reaction kinetics for the decomposition of materials of similar functional groups found in ZDDP, e.g. dimethyl and diethyl disulfide [21] and other groups under shear [22, 23].

The zero order of the slow initial reaction is in agreement with the in-situ AFM results reported by Gosvami et al. [1], which suggested that the ZDDP decomposes initially with a zero reaction rate $n = 0.12 \pm 0.11$, whereas as rubbing continues the reaction rate becomes $n = 0.22 \pm 0.02$, which suggests more complex reaction pathways during the decomposition of the ZDDP.

For the case of DDP, the fitting results indicate that, regardless of the applied contact pressure, the slow linear phase of the tribofilm formation follows a zero reaction order with $n = 0.047 \pm 0.01$. On the other hand, the fast logarithmic growth phase of the tribofilm follows a more complex reaction kinetics with $n = 0.52 \pm 0.07$.

The zero order of the slow initial reaction is in agreement with the in-situ AFM results regarding the ZDDP tribofilms as well as the previously reported data of ZDDP [1]. However, the fractional logarithmic rate is lower than the one found for the case of ZDDP, i.e. 0.77. The reaction order can be taken as a measure for the decomposition efficiency to form the bulk of the tribofilm, i.e. sulfides and phosphates. The low order indicates that the DDP decomposition process includes more side and intermediate reactions of possibly volatile products that consume part of the available DDP molecules to form species other than sulfides and

phosphates.

Conclusion

In summary, the kinetics of P-based antiwear additives were studies under different operating conditions of sliding speed, temperature and contact pressure. The results indicate that the decomposition reactions of the additives and the growth rate of their protective tribofilms are independent of the sliding speed and are only dependent on the scanning cycles. This suggests that the growth occurs cumulatively in a layer-by-layer fashion, i.e. every rubbing cycle regardless of its timing adds one layer of a certain thickness depending on the other operating conditions of temperature and contact pressure. The data suggest that temperature and contact pressure have an accelerating effect on the reaction kinetics, i.e. the higher the temperature or pressure the higher the increase in the growth rate. For the ZDDP, the effect of temperature and contact pressure seems to have an additive effect, e.g. the maximum growth rate occurs when temperature and contact pressure are both maximum. However, the formation rate of the DDP tribofilm increases over contact pressure exponentially compared to its linear growth over temperature. The activation energy of the ZDDP ranges from about 35 to 43 kJ/mol, which is nearly twice the value found for the DDP additive ranging from 10 to 25 kJ/mol. The relatively small energy barrier of the DDP decomposition makes it more susceptible to contact pressure than the larger barrier found for ZDDP. This suggests that the lack of zinc cations within the DDP molecules results in overall weaker bonds compared to the ZDDP molecules. The ZDDP decomposition and the growth of its phosphate-based tribofilms appear to follow first order reaction kinetics. However, in the case of DDP, it appears to follow more complex reaction pathways with a fractional kinetics order of 0.52 ± 0.07. The fractional order indicates that the DDP decomposition process includes more side and intermediate reactions of possibly volatile products.

Acknowledgements

This work is supported by EPSRC (grant number EP/R001766/1) and Marie Curie Initial Training Networks (grant number 317334).

References

(1) Gosvami, N.; Bares, J.; Mangolini, F; Konicek, A.; Yablon, D.; Carpick, R. Mechanisms of antiwear tribofilm growth revealed in situ by single-asperity sliding contacts. *Science* **2015**, *348*, 102–106.

(2) Dorgham, A; Neville, A; Ignatyev, K; Mosselmans, F; Morina, A An in situ synchrotron XAS methodology for surface analysis under high temperature, pressure, and shear. *Review of Scientific Instruments* **2017**, *88*, 015101.

(3) Zhang, Z; Najman, M; Kasrai, M; Bancroft, G.; Yamaguchi, E. Study of interaction of EP and AW additives with dispersants using XANES. *Tribology Letters* **2005**, *18*, 43–51.

(4) Kim, B.; Mourhatch, R.; Aswath, P. B. Properties of tribofilms formed with ashless dithiophosphate and zinc dialkyl dithiophosphate under extreme pressure conditions. *Wear* **2010**, *268*, 579–591.

(5) Dorgham, A.; Parsaeian, P.; Neville, A.; Ignatyev, K.; Mosselmans, F.; Masuko, M.; Morina, A. In situ synchrotron XAS study of the decomposition kinetics of ZDDP triboreactive interfaces. *RSC Advances* **2018**, *8*, 34168–34181.

(6) Kim, B.; Sharma, V.; Aswath, P. B. Chemical and mechanistic interpretation of thermal films formed by dithiophosphates using XANES. *Tribology International* **2017**, *114*, 15–26.

(7) Martin, J. M.; Onodera, T.; Minfray, C.; Dassenoy, F.; Miyamoto, A. The origin of anti-wear chemistry of ZDDP. *Faraday discussions* **2012**, *156*, 311–323.

(8) Willermet, P.; Dailey, D.; Carter, R.; Schmitz, P.; Zhu, W Mechanism of formation of antiwear films from zinc dialkyldithiophosphates. *Tribology International* **1995**, *28*, 177–187.

(9) Brizmer, V; Pasaribu, H.; Morales-Espejel, G. E. Micropitting performance of oil additives in lubricated rolling contacts. *Tribology Transactions* **2013**, *56*, 739–748.

(10) Lainé, E.; Olver, A.; Beveridge, T. Effect of lubricants on micropitting and wear. *Tribology International* **2008**, *41*, 1049–1055.

(11) Andersson, J.; Antonsson, M.; Eurenius, L.; Olsson, E.; Skoglundh, M. Deactivation of diesel oxidation catalysts: Vehicle-and synthetic aging correlations. *Applied Catalysis B: Environmental* **2007**, *72*, 71–81.

(12) API *Engine Oil Licensing and Certification System*; tech. rep. API 1509; American Petroleum Institute, 2014, pp 1–138.

(13) Nicholls, M. a.; Do, T.; Norton, P. R.; Kasrai, M.; Bancroft, G. Review of the lubrication of metallic surfaces by zinc dialkyl-dithiophosphates. *Tribology International* **2005**, *38*, 15–39.

(14) Parsaeian, P.; Ghanbarzadeh, A.; Wilson, M.; Van Eijk, M. C.; Nedelcu, I.; Dowson, D.; Neville, A.; Morina, A. An experimental and analytical study of the effect of water and its tribochemistry on the tribocorrosive wear of boundary lubricated systems with ZDDP-containing oil. *Wear* **2016**, *358*, 23–31.

(15) Qu, J.; Barnhill, W. C.; Luo, H.; Meyer III, H. M.; Leonard, D. N.; Landauer, A. K.; Kheireddin, B.; Gao, H.; Papke, B. L.; Dai, S. Synergistic Effects Between Phosphonium-Alkylphosphate Ionic Liquids and Zinc Dialkyldithiophosphate (ZDDP) as Lubricant Additives. *Advanced Materials* **2015**, *27*, 4767–4774.

(16) Burkinshaw, M.; Neville, A.; Morina, A.; Sutton, M. ZDDP and its interactions with an organic antiwear additive on both aluminium–silicon and model silicon surfaces. *Tribology International* **2014**, *69*, 102–109.

(17) Fatima, N.; Minami, I.; Holmgren, A.; Marklund, P.; Berglund, K.; Larsson, R. Influence of water on the tribological properties of zinc dialkyl-dithiophosphate and over-based calcium sulphonate additives in wet clutch contacts. *Tribology International* **2015**, *87*, 113–120.

(18) Zhang, J.; Yamaguchi, E.; Spikes, H. The antagonism between succinimide dispersants and a secondary zinc dialkyl dithiophosphate. *Tribology Transactions* **2014**, *57*, 57–65.

(19) Parsaeian, P.; Ghanbarzadeh, A.; Van Eijk, M. C.; Nedelcu, I.; Neville, A.; Morina, A. A new insight into the interfacial mechanisms of the tribofilm formed by zinc dialkyl dithiophosphate. *Applied Surface Science* **2017**, *403*, 472–486.

(20) Neville, A; Morina, A; Haque, T; Voong, M Compatibility between tribological surfaces and lubricant additives–how friction and wear reduction can be controlled by surface/lube synergies. *Tribology International* **2007**, *40*, 1680–1695.

(21) Adams, H.; Miller, B. P.; Kotvis, P. V.; Furlong, O. J.; Martini, A.; Tysoe, W. T. In situ measurements of boundary film formation pathways and kinetics: dimethyl and diethyl disulfide on copper. *Tribology Letters* **2016**, *62*, 12.

(22) Felts, J. R.; Oyer, A. J.; Hernández, S. C.; Whitener Jr, K. E.; Robinson, J. T.; Walton, S. G.; Sheehan, P. E. Direct mechanochemical cleavage of functional groups from graphene. *Nature communications* **2015**, *6*, 6467.

(23) Adams, H. L.; Garvey, M. T.; Ramasamy, U. S.; Ye, Z.; Martini, A.; Tysoe, W. T. Shear-induced mechanochemistry: pushing molecules around. *The Journal of Physical Chemistry C* **2015**, *119*, 7115–7123.

(24) Zhang, J.; Spikes, H. On the mechanism of ZDDP antiwear film formation. *Tribology Letters* **2016**, *63*, 1–15.

(25) Beyer, M. K. The mechanical strength of a covalent bond calculated by density functional theory. *The Journal of Chemical Physics* **2000**, *112*, 7307–7312.

(26) Shimizu, Y.; Spikes, H. A. The influence of slide–roll ratio on ZDDP tribofilm formation. *Tribology Letters* **2016**, *64*, 19.

(27) Gotsmann, B.; Lantz, M. A. Atomistic wear in a single asperity sliding contact. *Physical review letters* **2008**, *101*, 125501.

(28) Liu, J.; Notbohm, J. K.; Carpick, R. W.; Turner, K. T. Method for characterizing nanoscale wear of atomic force microscope tips. *ACS nano* **2010**, *4*, 3763–3772.

(29) Tran, R.; Xu, Z.; Balachandran Radhakrishnan, D. W.; Sun, W.; Persson, K. A.; Ong, S. P. Surface energies of elemental crystals. *Scientific data* **2016**, *3*, 160080.

(30) Hsu, S. M.; Gates, R. S. Effect of materials on tribochemical reactions between hydrocarbons and surfaces. *Journal of Physics D: Applied Physics* **2006**, *39*, 3128.

(31) Clasen, C.; Kavehpour, H. P.; McKinley, G. H. Bridging tribology and microrheology of thin films. *Appl. Rheol* **2010**, *20*, 196.

(32) Gosvami, N. N.; Nalam, P. C.; Exarhos, A. L.; Tam, Q.; Kikkawa, J. M.; Carpick, R. W. Direct torsional actuation of microcantilevers using magnetic excitation. *Applied Physics Letters* **2014**, *105*, 093101.

(33) Tysoe, W. On Stress-Induced Tribochemical Reaction Rates. *Tribology Letters* **2017**, *65*, 48.

(34) Ito, K.; Martin, J.-M.; Minfray, C.; Kato, K. Low-friction tribofilm formed by the reaction of ZDDP on iron oxide. *Tribology international* **2006**, *39*, 1538–1544.

(35) Ito, K; Martin, J.; Minfray, C; Kato, K Formation mechanism of a low friction ZDDP tribofilm on iron oxide. *Tribology transactions* **2007**, *50*, 211–216.

(36) Mosey, N. J.; Woo, T. K. Finite temperature structure and dynamics of zinc dialkyldithiophosphate wear inhibitors: a density functional theory and ab initio molecular dynamics study. *The Journal of Physical Chemistry A* **2003**, *107*, 5058–5070.

(37) Park, I.; Shirvanyants, D.; Nese, A.; Matyjaszewski, K.; Rubinstein, M.; Sheiko, S. S. Spontaneous and specific activation of chemical bonds in macromolecular fluids. *Journal of the American Chemical Society* **2010**, *132*, 12487–12491.

(38) Briscoe, B.; Evans, D. The shear properties of Langmuir-Blodgett layers. *Proceedings of the Royal Society of London. A. Mathematical and Physical Sciences* **1982**, *380*, 389–407.

(39) Sang, Y.; Dubé, M.; Grant, M. Thermal effects on atomic friction. *Physical review letters* **2001**, *87*, 174301.

(40) Liu, X.-Z.; Ye, Z.; Dong, Y.; Egberts, P.; Carpick, R. W.; Martini, A. Dynamics of atomic stick-slip friction examined with atomic force microscopy and atomistic simulations at overlapping speeds. *Physical review letters* **2015**, *114*, 146102.

(41) Li, Q.; Dong, Y.; Perez, D.; Martini, A.; Carpick, R. W. Speed dependence of atomic stick-slip friction in optimally matched experiments and molecular dynamics simulations. *Physical review letters* **2011**, *106*, 126101.

(42) Hammond, G. S. A correlation of reaction rates. *Journal of the American Chemical Society* **1955**, *77*, 334–338.